Dual Computational Systems in the Development and Evolution of Mammalian Brains

Nabil Imam[1,*], Matthew Kielo[1], Brandon M. Trude[1], and Barbara L. Finlay[2,*]

[1]School of Computational Science and Engineering, Georgia Institute of Technology, Atlanta, GA, USA
[2]Behavioral and Evolutionary Neuroscience Group, Department of Psychology, Cornell University, Ithaca, NY, USA

*Corresponding Authors. Emails: nimam6@gatech.edu, barbara.finlay@cornell.edu

Abstract

Analysis of brain volumes across mammalian taxonomic groups reveal a pattern of complementary and inverse covariation between major brain components, including a robust negative covariation between the limbic system and neocortex. To understand the computational basis of this covariation, we investigated the multidimensional representational space of task-optimized machine learning systems. We found that a smooth mapping of this space onto a two-dimensional surface leads to a characteristic layout depending on the structure of its information source. Visual, somatosensory and auditory systems develop ordered spatiotopic maps where units draw information from localized regions of the sensory input. Olfactory and relational memory systems, in contrast, develop fractured maps with distributed patterns of information convergence. Evolutionary optimization of multimodal systems result in inverse covariation between spatiotopic and disordered system components that compete for representational space. These results suggest that the observed pattern of covariation of brain components reflect an essential computational duality in brain evolution.

Keywords: development, evolution, computation, limbic system, neocortex, self-organizing maps

One entity in the vertebrate brain has attracted the attention of researchers for decades, but it has resolutely resisted definition, or even exact specification of its contents. The anatomical term "limbic system" designates the presence of a number of the entity's elements on the limbus, or edge of the embryonic lateral ventricle of the forebrain, including the rhinal and entorhinal cortices (variably, depending on each researcher's focus), the subicular cortices and hippocampus, the amygdala, septal and other basal forebrain nuclei, with the connections to the cingulate cortices of the neocortex often emphasized. The "rhinencephalon", smell-brain, features the olfactory system, the sensory receptors of main olfactory bulb and vomeronasal organ, and their primary targets, including primary olfactory cortex ("pyriform cortex"), the amygdala, additional basal forebrain nuclei of the olfactory tubercle and the parahippocampal gyrus, and the secondary targets of the hippocampus, thalamus and areas of neocortex as recruited. Those describing a memory-dedicated system will excise primary chemosensory and most basal forebrain nuclei from the group and add details and subdivisions to the hippocampus, entorhinal cortex and immediately interwoven cortex-like structures. Particularly in the field of neurology, the emotional sequelae of damage to collections of these regions were marked (e.g. "Kluver-Bucy syndrome", "septal rage").

Even with these disparate and often disjoint functions, integration over these nuclei and cortices was and is routinely emphasized. For example, "Papez's circuit", a collection of tracts often featured in medical textbooks, is so prominent it can be traced by blunt dissection, connecting the hippocampus via the fornix to the mammillary bodies of the hypothalamus, thence to the anterior nuclei of the thalamus, to limbic cortices and back to hippocampus. It's the rare current neuroscience textbook that fails to note the special emotional salience of olfactory memories. Unfortunately, one attempt to integrate over these diverse regions, Paul MacLean's "triune brain" theory, popularized in Carl Sagan's Dragons of Eden, persists to this day in the

evocation of "my lizard brain" to account for uncontrolled emotional excess by the utterly false evolutionary tale that reptiles have only brain up to and including the olfactory and emotional rhinencephalon, grown over later by the logical neocortex, reaching its full flower in humans.

Fortunately, theories much better integrated over evolutionary, embryonic, neurophysiological and neurologic reality were developed. Walle Nauta, saw the whole brain as characterized by two ascending systems, one, the ascending core, open, polysynaptic, concerned with evaluative sensation and physiological maintenance, and that integrated at the level of the hypothalamus and limbic regions, and a second fast-conducting, analytical (as in rapid skin sensation, vision and hearing), organized at the level of the thalamus and neocortex. The brain becomes integrated over these two systems for movement selection and affect in the basal ganglia of the forebrain. A separate thread ranks cortical structures across both limbic and neocortical origins in a hierarchy of prediction and control of emotional/physiological, motor and sensory states, choices and evaluation. A characterization of the forebrain based on developmental gene expression gives a better original segmentation, and characterization of changing segmental and neuronal fates as brains enlarge. In fact, the need for any complementary characterization of forebrain at all is called into question. To list just a few of the contradictions in the limbic/other cortex distinction: no empirical justification exists to view olfaction as more emotion-laden than the voices of significant others; the hippocampus gets rather little olfactory input in many mammals and can't be viewed as an olfactory structure; the hippocampus and neocortex both span the domains of emotion, event and sensorimotor world evaluation.

And yet, in a quite unexpected turn, the evolution and development of the vertebrate brain forces a two-systems view back into prominence. This is no invocation of the new brain-on-old brain layering of a scala naturae of fish, reptile, monkey and human – all vertebrates have essentially the same gross forebrain-to-spinal-cord segmentation, with no segments added on. Within those segments, the general functional commitment of regions remains remarkably stable, with the anterior-most and lateral-most regions of the embryonic neural plate destined to proliferate relatively the most in the larger brain. Rather, a strong pattern of complementary covariation between the cortical elements of the forebrain was first described quantitatively by Harry Jerison (though arguably misnamed) and has proven to be a volumetric distinction echoed between all large vertebrate taxonomic groups that have been studied, within taxonomic groups, and in individual variation within species, including our own. A push-pull relationship between the limbic system and the neocortex is evident in the data, with a volumetric expansion of one concomitant with a shrinkage of the other, after concerted allometric scaling is taken into account. We argue that this two-systems organization is characterized by distinct connectivity patterns in the component networks. The olfactory system and hippocampus have as their base a widely distributed patten of axon extension, whereby distributed neural activity patterns identify a particular odorant in the case of the olfactory structures, and a unique event in the case of the hippocampus. The neocortex, in contrast, preserves local spatial relationships in the projections of its subregions, cortical areas onto each other. In most of the lateral convexity of the cortex, the dimensions that are mapped between areas represent egocentric space, over several sensory modalities and the motor modality, with cortical maps maintaining nearest neighbor relationships of the sensory and motor surfaces. In part of the cortex (the temporal lobe in humans), spatially ordered cortical projections are employed for non-egocentric mapping, as in tonotopy in auditory cortical representations, or the often-hybrid representations of faces, scenes, words and concepts.

We propose that the reason for the different patterns of axonal projections in the two systems is a computational one, that optimal representations of the associated modalities are achieved with distinct network architectures that induce system-specific inductive biases. To investigate, we projected the representational space of task-optimized artificial neural networks to a two-dimensional model cortical sheet using self-organizing maps. We found that networks optimized for visual, tactile and auditory representations converge to orderly spatiotopic maps that maintain nearest neighbor relationships of the input array, resembling sensory maps and connectivity profiles in the neocortex. In contrast, networks optimized for olfactory and relational memory representations evolved fractured maps with distributed connectivity profiles resembling axon distribution patterns of the olfactory-limbic system. Using evolutionary optimization, we optimized a multimodal network consisting of two subnetworks, one with spatiotopic and the other with distributed architecture. Selecting for different task objectives, we found an inverse relationship between the two sub-

networks, resembling the inverse covariation between olfactory-limbic and neocortical system sizes observed across species. Our results provide a computational account of a 550-million-year-old essential duality of the vertebrate brain.

Neocortex and Limbic System Covariation

We used data collected for allometric analysis of brain structures in 183 mammalian species across 10 taxonomic groups including *Homo sapiens*. Figure 1a plots the size (volume) of the neocortex against the size of the olfactory system for each species; the size of each structure is normalized with respect to core brain components. A robust negative correlation between the two systems is evident in the plot. Insectivores (hedgehogs, tree shrews, frogs) have relatively large olfactory systems and small neocortices, whereas primates, pinnipeds, ungulates and carnivores, and the manatee have reduced olfactory systems and enlarged neocortices. This inverse relationship can be partly understood by the dominant sensory systems of the taxonomic groups involved. Insectivores, or small insect-eating mammals, are often nocturnal, rely on olfactory cues for foraging, and have relatively large olfactory bulbs and olfactory cortices. In contrast, primates are highly visual, with a large fraction of the neocortex taken up by primary and extrastriate visual cortices. This contrast between olfaction and vision can be seen throughout the vertebrate lineage, in aquatic species, reptiles, birds, and mammals [1], and is so striking that it can be seen in whole brains. Figure 1b shows a lateral view of the brains of an owl monkey and an agouti. The brains are similar in volume, but the difference in the relative sizes of the neocortex and the olfactory system is apparent, with the neocortex in the primate obscuring all other components from view, including the cerebellum, which is equal in size in both brains.

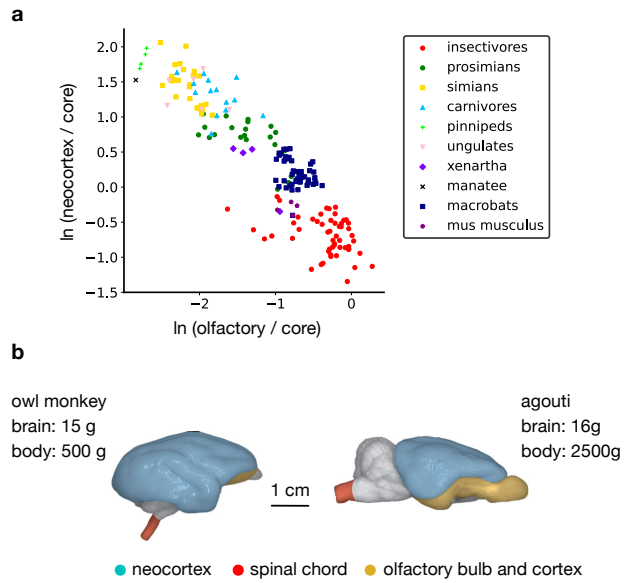

Figure 1: (a) Volume of the neocortex (y-axis) plotted against the volume of the olfactory system (x-axis) for 183 mammalian species across 10 taxonomic group. The volumes are expressed as a fraction of the total volume of a core set of brain components (medulla, mesencephalon, diencephalon, striatum), in natural log scale. (b) The brains of an owl monkey and an agouti. The owl monkey is from the simian taxonomic group in subplot *a*, and the agouti is from the insectivore group. The neocortex takes up a disproportionate amount of space in the owl monkey whereas the olfactory bulb and cortex takes up a significant fraction in the agouti.

Figure 2a depicts a coronal section of the forebrain at the posterior thalamus level in a squirrel monkey and a nine-banded armadillo (from the Xenarthra taxonomic group in the bottom-right corner of Figure 1a). The relatively larger olfactory cortices in the armadillo is expected from an olfaction vs vision account of sensory specialization, but the drastically enlarged hippocampus is striking. Across taxonomic groups, the hippocampus has a strong positive correlation with the olfactory system, as shown in Figure 2b, that contrasts with the inverse relationship between the olfactory system and neocortex in Figure 1a. Why does the size of the hippocampus positively covary with that of the olfactory system? An explanation based on strong interlinking between the two structures is not adequate as only a small fraction of the input to the hippocampus is olfactory [2]. The hippocampus integrates multiple streams of information, including those originating in the neocortex, and cannot be viewed as an olfactory structure. In the following sections we argue that this covariation between the olfactory system and the hippocampus reflect a shared computational architecture which is distinct from the architecture of the neocortex.

In addition to the hippocampus, all other limbic system components, including the amygdala, septum, and

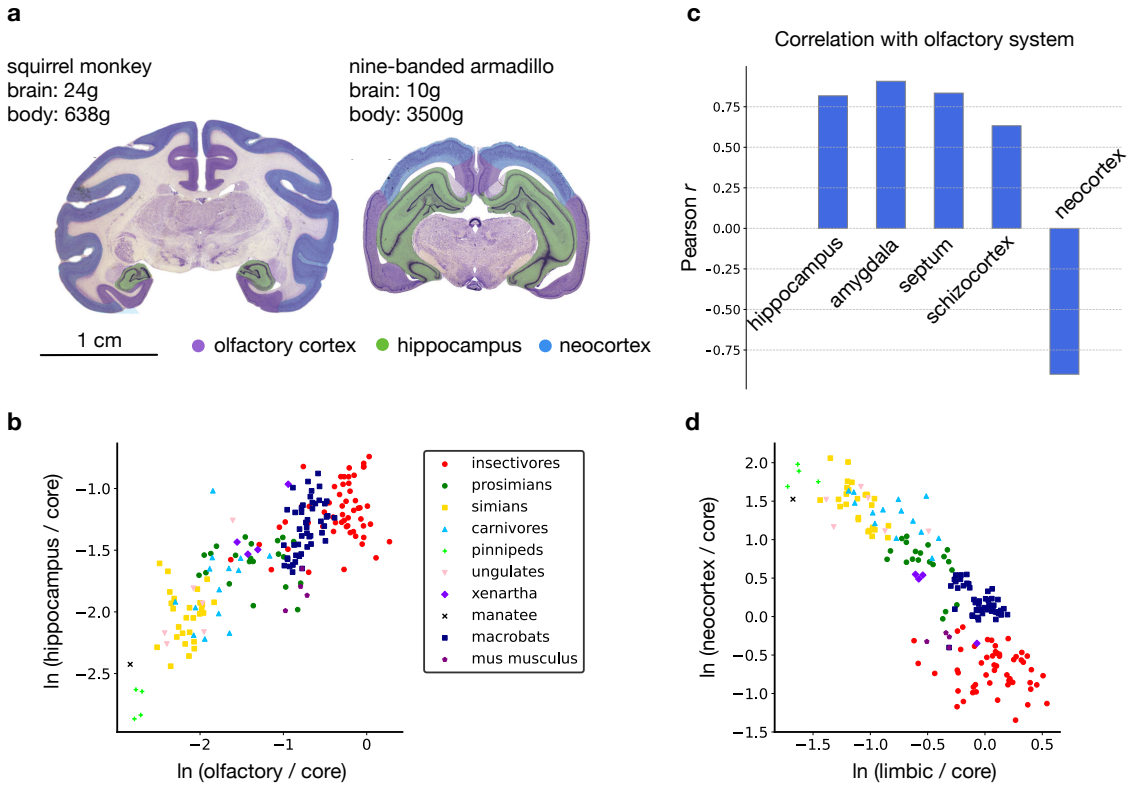

Figure 2: (a) Cross-section of the brain of a squirrel monkey and a nine-banded armadillo showing an enlarged neocortex in the monkey and an enlarged olfactory cortex in the armadillo. Note the expansion of the hippocampus in the armadillo. (b) Normalized volumes of the hippocampus plotted against that of the olfactory system across species (Pearson r = 0.82). (c) All limbic system components have strong positive covariation with the olfactory system. In contrast, the neocortex has strong negative covariation. Shown are the Pearson correlation coefficients between the normalized volumes of each structure and that of the olfactory system across species. Schizocortex includes entorhinal, perirhinal, presubicular and parasubicular cortices. Amygdala volumes were separately available for 103 of the 183 species analyzed. (d) Normalized volume of the neocortex plotted against that of the limbic system (sum of normalized volumes of all limbic system components) across species. A robust negative covariation is evident (Pearson r = -0.84).Images in subplot *a* are from the Comparative Mammalian Brain Collections, www.brainmuseum.org, property of the University of Wisconsin and Michigan State Comparative Mammalian Brain Collections, funded by the National Science Foundation and the National Institutes of Health.

schizocortex, positively covary with the olfactory system (Figure 2c) and with each other. This concerted change of limbic system components along with their inverse covariation with the neocortex (Figure 2d) suggests a two-systems view of the macroscale organization of the brain. This view is reinforced by the fact that development keeps the two systems distinct, both in the their germinal zones [3] and in the later expression of transcription factors [4], suggesting distinct developmental rules of network formation.

Structure of Sensory and Cognitive Maps

Optimized representations and information structure. To investigate the reasons underlying the pattern of covariation in brain evolution, we sought to understand the structure of distinct information sources driving brain computation and their optimal representations. For this purpose, we assessed the multidimensional representational space of modern machine learning systems optimized for one of four sensory modalities – vision, audition, somatosensation and olfaction – followed by a system optimized for relational

memory. The sensory systems consist of the following artificial neural network architectures pre-trained on large data corpora **(1)** ResNet trained on images from the ImageNet database [5,6], **(2)** wav2vec 2.0 trained on natural speech from the Libri speech corpus [7,8], **(3)** a convolutional architecture trained on a dataset of tactile signals of the human grasp [9], and **(4)** an olfactory systems model trained on olfactory receptor neuron activation profiles [10]. These networks show strong correspondence to neural activity and structural connectivity patterns in the brain under certain parameter regimes [6, 8–10]. Training optimizes network connection weights, and subsequently, the networks embed manifolds of stimulus feature information in their connectivity.

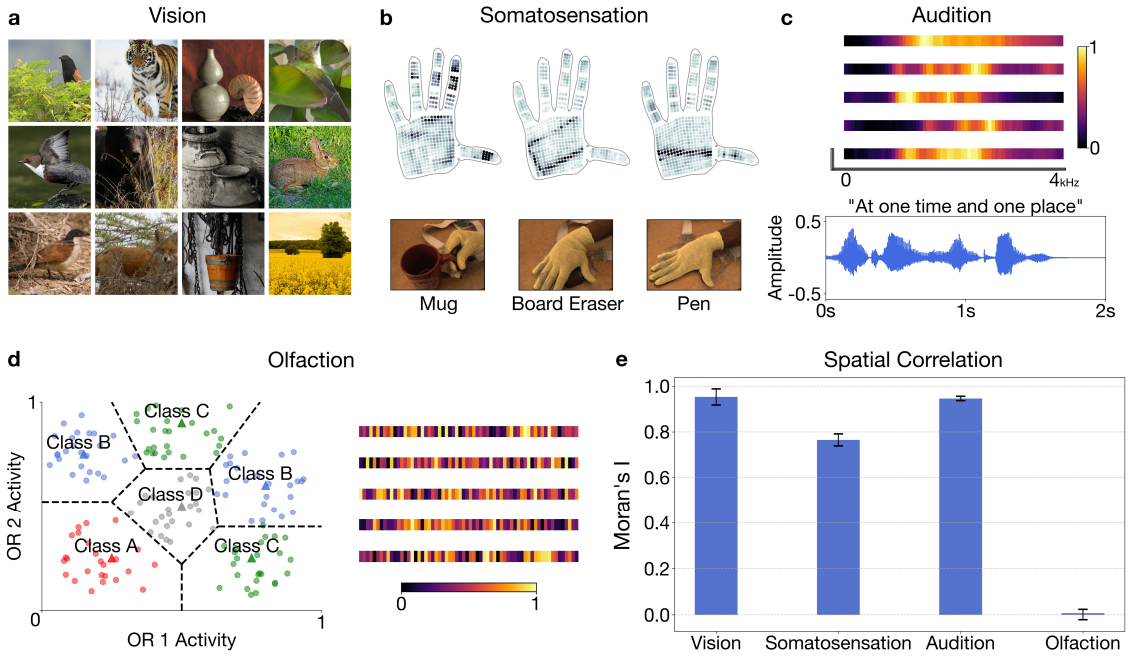

Figure 3: Information sources of four sensory modalities. (a) Samples from the ImageNet dataset. ImageNet images are characterized by spatial correlation visible in the form of contrastive backgrounds, repeating textures, and distinct natural shapes. (b) Top: visualizations of pressure readouts from the tactile glove dataset [9]. Bottom: perspective images showing the creation of each sample. Activated regions of the tactile glove are highly localized, as clusters of adjacent sensors respond to pointwise contact with the object being classified. (c) One-dimensional cochleagram slices (top) and time-amplitude representation of a single sample (bottom), each from the LibriSpeech ASR corpus. In the cochleagram slices, frequency bands associated with human speech form localized patterns. (d) Left: subset of 150 synthetic odors from the Wang et al dataset [10] showing activation values of two olfactory receptor neurons (ORNs). Each odor sample is encoded by 50 ORNs in the dataset. Individual odors are classified by their proximity to two prototype odors (triangles) which are distributed across the full range of possible values and exhibit minimal local spatial correlation. Right: ORN activation profiles of five sample odors from the dataset. (e) Barplot showing spatial autocorrelation (Moran's I) across the aforementioned datasets. Moran's I is the ratio of the spatially weighted covariance to the overall variance, normalized by the number of observations and the sum of the spatial weights. This metric is expressed in a range from -1 to 1, where positive values indicate increasingly strong local similarity, values near zero suggest random spatial patterns, and negative values indicate strong local dissimilarity.

The data used to optimize each model is depicted in Figures 3a-d. We observe a dichotomy in the structure of information across modalities, with visual, auditory, and somatosensory data showing pronounced spatial structure, as measured by spatial autocorrelation (Moran's I, Figure 3e), and olfactory data lacking any such structure. Coarse-scale chemotopy in olfactory receptor neuron population representations have been proposed in some studies [11] and debated in others [12], but it is clear that they lack the fine-grained spatial order characteristic of primary visual, somatosensory and auditory representations [12–15]. We argue that this dichotomy in the structure of information sources underlies the two-systems architecture that we proposed, each system pre-configured with knowledge of the core statistical structure in their input.

Spatiotopic and disordered maps. After optimization of network parameters in the models, network activity constitutes an optimized population code of stimulus features across a multi-dimensional representational space. A prevailing theoretical account of cortical organization posit that such multi-dimensional feature spaces are represented in two-dimensional cortical surfaces in a manner that preserves similarity between feature representations [16–18]. Similar features are represented in nearby locations on the cortical surface to aid efficient similarity-dependent computations. Following this account, we constructed Kohonen self-organizing maps (SOMs) to represent the optimized feature spaces of our models on a two-dimensional cortex-like surface. We considered the organization of primary sensory maps that are in place early in brain development and whose activity drive areal organization across the system [19, 20]. Specific layers of our models show strongest correspondence to activity in primary sensory areas and we construct SOMs using activity in these layers [6, 8–10].

Figure 4a shows the maps that developed in each modality, highlighting two contrasting structures. Visual, auditory and somatosensory maps converged to orderly representations that maintain nearest neighbor relationships of the sensory surface resembling spatiotopic organization that characterizes the entire neocortex. Olfactory maps, in contrast, developed fractured representations akin to disordered chemotopy in the olfactory bulb and cortex. We quantified the degree of global spatial order in each map by computing the mean Euclidean distance between each unit's preferred stimulus and that of its adjacent units, normalized by the expected distance in a random arrangement and negated to result in an order metric. This results in an index that ranges from 0 (low order) to 1 (high order). We measured values of 0.91, 0.89 and 0.89 for visual, somatosensory and auditory maps respectively, and 0.08 for olfactory maps.

We then assessed the receptive fields of individual SOM units and found that visual, somatosensory and auditory units draw information from localized regions of the sensory surface, whereas olfactory units sample across distributed parts (Figure 4b), recapitulating a central distinction between afferent projection patterns in primary olfactory cortex and primary sensory areas of neocortex. We measured the degree of locality of the receptive fields by computing the spatial autocorrelation (global Moran's I) of representative SOM unit receptive fields, again resulting an index that ranges from 0 (low locality) to 1(high locality). We found locality indices of 0.99, 0.87 and 0.89 for vision, somatosensation and audition respectively, and 0.06 for olfaction. We also found that this pattern of information convergence arises within unstructured (fully-connected) networks solely as a consequence of gradient-based optimization of information representation without prespecified network structure. Overall, the contrasting structure of information representation between the spatiotopic and olfactory modalities mirrors the dual structure of their information sources (Figure 3) and underscores a pronounced duality in the organization of optimal sensory representations.

Relational memory. We next assessed representations in the Tolman-Eichenbaum Machine (TEM), an artificial neural network for relational inferences modeled on computations in the hippocampus and entorhinal cortex [21]. The network was trained to learn conjunctions of perceptual and structural representations and developed a cognitive map via which relationships between objects and their spatial or abstract locations were inferred (Figure 5a). Activity within the network resembled activity patterns in spatial and non-spatial cell types in the hippocampus and entorhinal cortex, as well as their structural remapping under new stimuli [21]. We projected the conjunctive representations of this model onto a two-dimensional surface using a SOM and compared its structural features to the sensory systems maps of Figure 4.

As in the olfactory maps, hippocampal maps developed fractured representations that lack global spatial

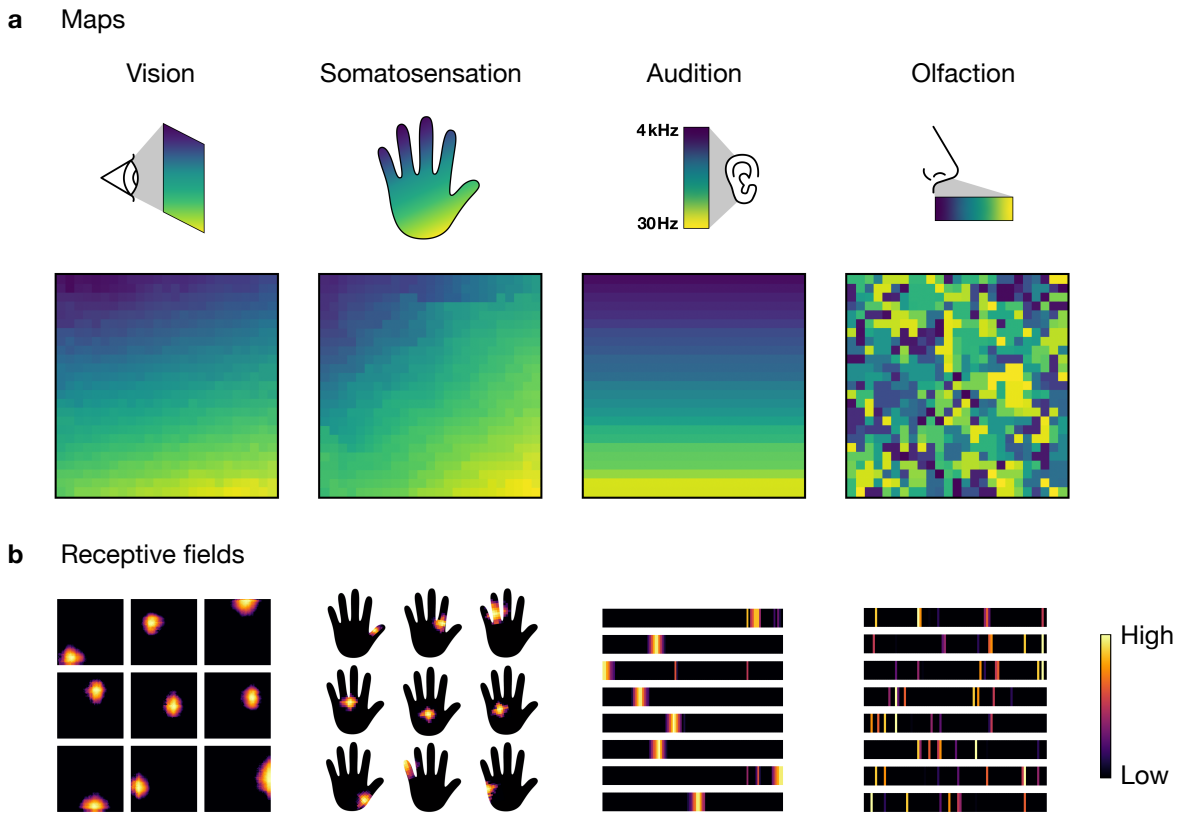

Figure 4: (a) Model cortical sheets constructed by projecting the multidimensional representational space of task-optimized artificial neural networks to two-dimensional surfaces using distance-preserving projections [18]. Models of four sensory systems were constructed. The top row depicts the sensory input colored by location. The bottom row shows maps of the sensory input on the model sheets. Each sheet consists of 25 x 25 units. Each unit is colored according to the input location that maximally activates the unit. The gradual transition of colors in visual, somatosensory, and auditory representations indicate a smooth mapping of the input space on the cortical surface. No such mappings were found for olfactory representations. (b) Example receptive fields of model units indicating the degree to which each region of the input space activates a unit. Receptive fields in vision, somatosensation and audition are spatially localized whereas those in olfaction are spatially distributed.

order, with SOM units drawing information from distributed parts of the TEM's input (Figure 5d-e), resembling sparse and distributed coding in the hippocampus [22,23]. We compared map indices across models and found a grouping between olfactory and hippocampal representations, both having low indices for spatiotopic order and receptive field locality in contrast to the maps of the other sensory systems (Figure 5f-g).

The hippocampus representation in the TEM model arose within a recurrent neural network that learned associations between sensory and locational representations. This network was initialized without any pre-configured structure in its connectivity, both in the afferent and recurrent connectivity matrices. Similarly, the olfactory network model was not pre-specified with prior structure and instead developed sparse distributed organization over the course of gradient-based optimization for olfactory signal recognition. We investigated whether pre-specifying particular patterns of connectivity prior to optimization affected performance of these two networks. Specifically, we pre-configured local structure in those connections akin to local structure in the visual, somatosensory and auditory systems, and found that it resulted in a significant degradation of performance. This indicates that olfactory and hippocampal computations both benefit from inductive biases that are distinct from those of the other sensory modalities.

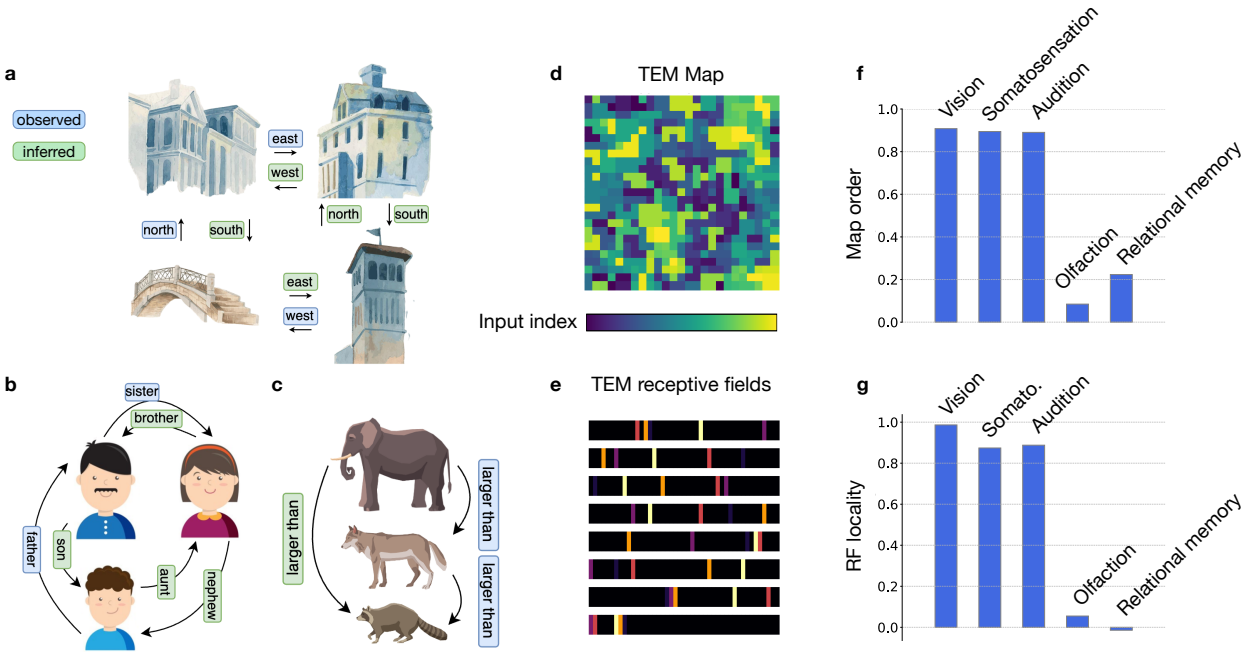

Figure 5: The Tolman-Eichenbaum Machine (TEM) learns relational structure of a problem and uses that knowledge to make quick inferences in new problem instances. Relational structure exists in many situations, for example (a) spatial reasoning, (b) social hierarchies and (c) transitive inference. The TEM infers the green relationships after observing only the blue ones using a connectionist model of the hippocampus and entorhinal cortex. Figures adapted from [21]. (d) Hippocampal activity of the TEM is projected to a two-dimensional surface using distance-preserving projections. Shown is a surface consisting of 25x25 units, where each unit is colored according to the location of the input that maximally activates that unit. The disordered map resembles the olfactory map of Figure 4a. (e) Example receptive fields of hippocampal units in the TEM. The receptive field of a unit (1D horizontal bar) shows the degree to which each region of the input activates that unit. The spatially dispersed receptive fields resemble those of the olfactory map in Figure 4b. (f-g) Indices of map order and receptive field locality showing that hippocampal relational memory and olfactory representations have distinct structure compared to the spatiotopic sensory systems.

Evolution of a dual computational system

The structure of optimal representations discussed so far mirrors the structure of primary sensory representations in the brain in place early in development. This pre-configuration of network architectures prior to stimulus exposure serves subsequent computations by encoding knowledge of the structure of expected stimuli in network connectivity. What developmental factors shape this connectivity and what axes of variations are offered up to natural selection? To investigate this in the context of our results, we configured a dual-systems architecture consisting of two subnetworks, one with spatiotopic and the other with distributed organization drawing input from five sources of information – visual, somatosensory and auditory sources providing input to the spatiotopic network, and olfactory and hippocampal sources to the distributed network (Figure 6a). Units within the spatiotopic and distributed networks were allocated equally among their constituent components. We asked how these networks may co-vary under selection pressures along a single dimension of variation – the location of the boundary dividing the spatiotopic and distributed subnetworks. The boundary determines the number of units, or the amount of computational resources, allocated to each modality and its variation accounts for a minimal degree of stable developmental control of tissue allocation (Figure 6b). We used an evolutionary algorithm to optimize the position of this boundary under a selection criterion defined by a parameter s that takes a value between 0 and 1; a low value of s selects for olfaction and a high value selects for vision. We initialized a population of networks each with an even allocation of units between the spatiotopic and distributed networks, and ran the evolutionary algorithm for fifty generations.

At each step, the location of the boundary in each network is varied uniformly at random and the networks with highest task performance are selected; task performance is a combination of olfactory and visual signal identification, as defined by the parameter s. The algorithm optimized the performance of the networks across iterative steps of variation and selection.

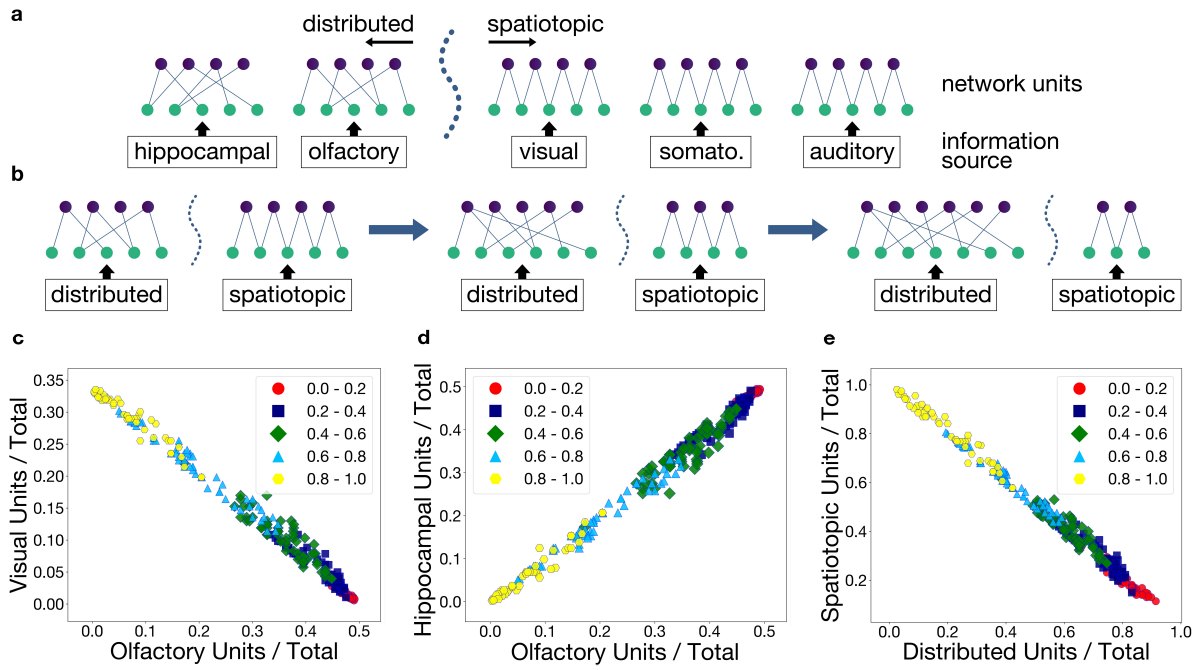

Figure 6: An evolutionary algorithm accounts for patterns of covariation among brain components. (a) A dotted boundary separates two networks with distributed connections at their input layers from three networks with spatiotopic (local) connections at their inputs. Shifting this boundary adjusts the number of units allocated to each side proportionally. New generations of networks are produced by randomly stepping the boundary in the direction associated with the fittest survivors from the previous generation. (b) Depiction of selecting for olfaction. The boundary shifts in a direction that expands the distributed network resulting in a larger allocation of network units to the constituent components. (c) Allocation percentages to the visual and olfactory components after 50 generations. Points are categorized by groupings of "s" values in a range from 0 to 1 where s is the weight assigned to the test performance of vision when calculating the fitness of a given network. (d) Similar to subplot c, but showing the allocation percentages between the hippocampal and olfactory components of the network.(e) Displays the combined unit allocations for the visual, somatosensory, and auditory portions of the network (y-axis) against the combined allocations for the olfactory and hippocampal portions (x-axis) after 50 generations. The trends in subplots c-e are similar to those observed across species.

Figure 6c shows the outcome of the evolutionary optimization process for different values of s. When olfactory performance was selected for (low values of s), the number of units allocated to olfaction increased at the expense of vision, and vice-versa (high values of s), recounting the olfaction vs vision account of sensory specialization (Figure 1). We also found that instead of singular expansion of the selected component, a concerted change in the size of all components took place, with olfactory and hippocampal network sizes positively covarying with one another and inversely covarying with the sizes of the spatiotopic networks (Figure 6d-e). These results show that a minimal degree of developmental control is sufficient to account for overall patterns of covariation observed across species (Figures 1 and 2). A segmental 'prosomeric' structure of the forebrain defined by domains of regulatory gene expressions suggest a mechanism of this nature [24,25].

When evolution selects for brain components, it selects for function that arises from underlying computational processes. Particular computations are aided by specific features of network architectures and

representational schemes, the spatiotopic and distributed networks discussed here being examples from what may be an abundant space of architectural priors exploited in brain computation. Variations in network organization offered up to natural selection are shaped by developmental processes and thus constrained by directions of variation under developmental control. These 'units of development' might not precisely correspond to the function that is selected for, and the outcome of selection is likely a result of specific functional demands and available developmental variation, mediated strongly by metabolic costs and other contingencies [2]. The results presented here suggest that the pattern of covariation between the limbic system and the neocortex observed across species is a consequence of developmental control of tissue allocation between two computational systems offered as loci of selection. Despite the diversity of limbic system function, a common computational architecture and coarse developmental structure underlies concerted variation of its components. Selecting for one causes the selection of all, with pleiotropic effects on behavior.

Acknowledgments

This work was supported by NSF grants 2223811 and 2319060 to NI.

References

[1] M. A. MacIver and B. L. Finlay, "The neuroecology of the water-to-land transition and the evolution of the vertebrate brain," *Philosophical Transactions of the Royal Society B*, vol. 377, no. 1844, p. 20200523, 2022.

[2] R. Reep, B. Finlay, and R. Darlington, "The limbic system in mammalian brain evolution," *Brain, behavior and evolution*, vol. 70, no. 1, pp. 57–70, 2007.

[3] R. Nieuwenhuys and L. Puelles, *Towards a new neuromorphology.* Berlin, Germany: Springer, 2015.

[4] P. Levitt, "A monoclonal antibody to limbic system neurons," *Science*, vol. 223, no. 4633, pp. 299–301, 1984.

[5] K. He, X. Zhang, S. Ren, and J. Sun, "Deep residual learning for image recognition," in *Proceedings of the IEEE conference on computer vision and pattern recognition*, 2016, pp. 770–778.

[6] E. Margalit, H. Lee, D. Finzi, J. J. DiCarlo, K. Grill-Spector, and D. L. Yamins, "A unifying framework for functional organization in early and higher ventral visual cortex," *Neuron*, 2024.

[7] A. Baevski, Y. Zhou, A. Mohamed, and M. Auli, "wav2vec 2.0: A framework for self-supervised learning of speech representations," *Advances in neural information processing systems*, vol. 33, pp. 12 449–12 460, 2020.

[8] Y. Li, G. K. Anumanchipalli, A. Mohamed, P. Chen, L. H. Carney, J. Lu, J. Wu, and E. F. Chang, "Dissecting neural computations in the human auditory pathway using deep neural networks for speech," *Nature Neuroscience*, vol. 26, no. 12, pp. 2213–2225, 2023.

[9] S. Sundaram, P. Kellnhofer, Y. Li, J.-Y. Zhu, A. Torralba, and W. Matusik, "Learning the signatures of the human grasp using a scalable tactile glove," *Nature*, vol. 569, no. 7758, pp. 698–702, 2019.

[10] P. Y. Wang, Y. Sun, R. Axel, L. Abbott, and G. R. Yang, "Evolving the olfactory system with machine learning," *Neuron*, vol. 109, no. 23, pp. 3879–3892, 2021.

[11] K. Mori, Y. K. Takahashi, K. M. Igarashi, and M. Yamaguchi, "Maps of odorant molecular features in the mammalian olfactory bulb," *Physiological Reviews*, vol. 86, no. 2, pp. 409–433, 2006.

[12] T. A. Cleland, "Early transformations in odor representation," *Trends in Neurosciences*, vol. 33, no. 3, pp. 130–139, 2010.

[13] V. N. Murthy, "Olfactory maps in the brain," *Annual Review of Neuroscience*, vol. 34, no. 1, pp. 233–258, 2011.

[14] E. R. Soucy, D. F. Albeanu, A. L. Fantana, V. N. Murthy, and M. Meister, "Precision and diversity in an odor map on the olfactory bulb," *Nature Neuroscience*, vol. 12, no. 2, pp. 210–220, 2009.

[15] R. M. Blazing and K. M. Franks, "Odor coding in piriform cortex: mechanistic insights into distributed coding," *Current Opinion in Neurobiology*, vol. 64, pp. 96–102, 2020.

[16] T. Kohonen, "Self-organized formation of topologically correct feature maps," *Biological cybernetics*, vol. 43, no. 1, pp. 59–69, 1982.

[17] R. Durbin and G. Mitchison, "A dimension reduction framework for understanding cortical maps," *Nature*, vol. 343, no. 6259, pp. 644–647, 1990.

[18] F. R. Doshi and T. Konkle, "Cortical topographic motifs emerge in a self-organized map of object space," *Science Advances*, vol. 9, no. 25, p. eade8187, 2023.

[19] N. Imam and B. L. Finlay, "Self-organization of cortical areas in the development and evolution of neocortex," *Proceedings of the National Academy of Sciences*, vol. 117, no. 46, pp. 29 212–29 220, 2020.

[20] M. Arcaro and M. Livingstone, "A whole-brain topographic ontology," *Annual Review of Neuroscience*, vol. 47, 2024.

[21] J. C. Whittington, T. H. Muller, S. Mark, G. Chen, C. Barry, N. Burgess, and T. E. Behrens, "The Tolman-Eichenbaum machine: unifying space and relational memory through generalization in the hippocampal formation," *Cell*, vol. 183, no. 5, pp. 1249–1263, 2020.

[22] S. N. Chettih, E. L. Mackevicius, S. Hale, and D. Aronov, "Barcoding of episodic memories in the hippocampus of a food-caching bird," *Cell*, vol. 187, no. 8, pp. 1922–1935, 2024.

[23] S. Srinivasan and C. F. Stevens, "Scaling principles of distributed circuits," *Current Biology*, vol. 29, no. 15, pp. 2533–2540, 2019.

[24] J. L. Rubenstein, S. Martinez, K. Shimamura, and L. Puelles, "The embryonic vertebrate forebrain: the prosomeric model," *Science*, vol. 266, no. 5185, pp. 578–580, 1994.

[25] L. Puelles, "An illustrated summary of the prosomeric model," *Frontiers in Mammal Science*, vol. 3, p. 1456996, 2024.